

# Maximum Power Search in Wind Turbine Based on Fuzzy Logic Control

**Evgenije Adzic\*, Zoran Ivanovic\*, Milan Adzic\*\*, Vladimir Katic\***

\* Faculty of Technical Sciences, Novi Sad, Serbia

\*\* Polytechnical Engineering College, Subotica, Serbia

evgenije@uns.ns.ac.yu, zorani@uns.ns.ac.yu, adzicm@vts.su.ac.yu,

katav@uns.ns.ac.yu

---

*Abstract: This paper describes fuzzy logic control of induction generator speed in wind turbine application. The aim of fuzzy controller is to establish maximum power delivery to the grid from available wind power. Fully-controlled wind turbine which consists of induction generator and back-to-back converter is under estimate. This configuration has full control over the electrical torque, full control of the speed, and also supports reactive power compensation and operation under grid disturbances. Fuzzy logic control algorithm has been applied and validated by detailed simulation in MATLAB/Simulink. All system components have been described in detail.*

---

## 1 Introduction

Increasing environmental concern during the 20<sup>th</sup> Century has moved the research focus from conventional electricity sources to renewable and alternative energy solutions. A number of renewable power generation sources exist, such as wind energy, solar energy, wave energy, hydro power and more sophisticated systems based on hydrogen. In renewable power generation, wind energy has been noted as the fastest-growing energy technology in the world. This is due to the fact that world has enormous resources of wind energy. It has been estimated that tapping barely 10% of the wind energy available could supply all the electricity needs of the world. Moreover, recent technological advances in variable-speed wind turbines, power electronics, drives, and controls have made wind energy competitive with conventional coal and natural gas power.

One of the problems of wind energy is that its availability is sporadic, and therefore it needs to be backed by other power sources, in order to avoid instability of the power system. Due to this, wind turbines are used as additional electrical energy sources among already installed conventional sources.

In the early years of the development, fixed speed wind turbines were the most installed wind turbines. They are equipped with an induction generator connected directly to the grid without converter. With this configuration it is not possible to extract all available wind energy. Power electronics makes it possible to apply the variable speed concept. By introducing variable speed operation, it is possible to continuously adapt the rotational speed of the wind turbine to the wind speed in a way that the turbine operates at its highest level of aerodynamic efficiency. Due to this advantage, power of wind turbines has been increased and variable speed wind turbines became the predominant choice for MW-scale turbines today. At the beginning, variable speed wind turbine concept with doubly fed induction generator and partial-scale back-to-back converter on the rotor circuit were most popular. This is due the fact that the partial-scale power converter is typically only 30% of the power fed to the electrical grid. This makes this concept attractive from an economic point of view.

In the past few years, price of the power electronics equipment dropped dramatically which put out the wind turbine configuration with squirrel-cage induction generator and full-scale back-to-back converter in the first plan. The main advantage of this configuration is the usage of standard and robust induction generator. This concept has full control over the electrical torque, full control of the speed range from 0% to the 100% of the synchronous speed, and also it supports reactive power compensation, smooth grid connection and proper operation in the case of grid disturbances (for example in the case of voltage sags). This configuration is shown in Fig. 1.

This paper deals with obtaining the proper algorithm in order to extract maximum power from available wind. To carry out this, fuzzy logic control of generator side converter and thus control of generator speed was used [3]. The advantages in using fuzzy logic controller against standard PI controllers, are pointed out in better response to frequently changes in wind speed.

First part of the paper gives general notes about wind energy and emphasizes what is needed to work at turbine maximum output power operating point. Second part explains control system for wind turbine with full-scale back-to-back converter. Third part introduce fuzzy logic controller which will track wind speed in order to extract maximum power. At the end of the paper simulation results verifies this optimum control.

## **2 Wind Energy**

Upon interaction of the wind and the turbine, power which is passed to the generator through turbine could be expressed by equation (1) [3, 4]:

$$P_{TUR} = \frac{1}{2} \cdot \rho \cdot A \cdot V_w^3 \cdot C_p(\lambda) \quad (1)$$

where are:

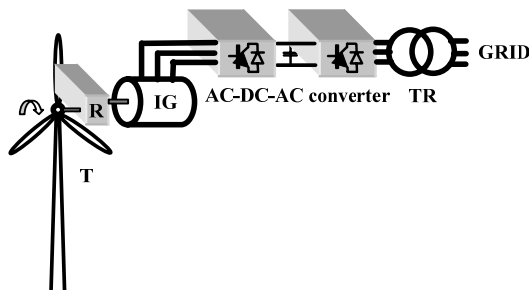


Figure 1

Wind turbine with full-scale back-to-back converter

- $\rho$  - air density
- $A$  - area covered with turbine blades
- $V_w$  - wind speed
- $C_p(\lambda)$  - turbine power coefficient
- $\lambda = \omega_{tur} \cdot R_{tur} / V_w$  - tip speed ratio
- $\omega_{tur}$  - turbine angular speed
- $R_{tur}$  - turbine radius

Set of turbine power curves are given in Fig. 2. It could be noticed that there is the operating point of maximum power delivery for each wind speed. The main goal of the controller is to run wind turbine generator at that operating point. These set of curves could be replaced with only one diagram which gives dependence of wind turbine power related to parameter  $\lambda$ , through turbine power coefficient marked as  $C_p(\lambda)$ . Particularly, the wind turbine is characterized by the power coefficient  $C_p(\lambda)$  (see Fig. 3), which is defined as the ratio of actual delivered power to the free stream power flowing through a same but uninterrupted area. The tip speed ratio  $\lambda$ , is the ratio of turbine speed at the tip of a blade to the free stream wind speed. It could be noticed from Fig. 3 that there is the optimal tip speed ratio  $\lambda_{opt}$ , which has to be maintained in order to extract maximum power from the wind.

Fuzzy logic controller (FLC) is used in order to achieve maximum power delivery for each wind speed and to have more robustness [1, 2]. Maximum output power operating point deviates from the maximum torque point. The torque follows the square-law characteristics and the output power follows the cube law. This means that under light load conditions, additional generator magnetic flux controller is needed in order to achieve more power efficiency, by reducing the iron losses. This controller is not investigated in this work.

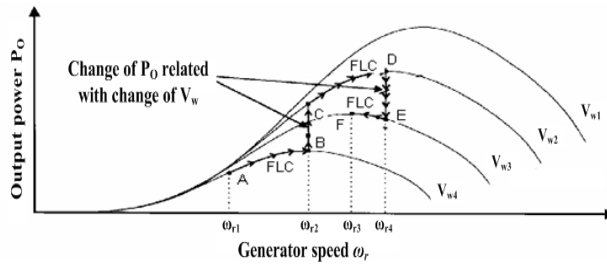


Figure 2

Set of turbine power curves related with generator speed, for different wind velocities

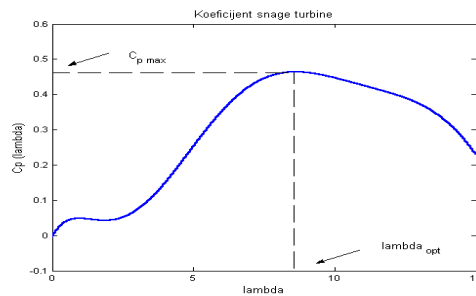


Figure 3

Power coefficient  $C_p(\lambda)$  related with tip-speed ratio  $\lambda$

### 3 Modeling of Wind Turbine Control System

Wind turbine control block diagram is shown in Fig. 4. The system consists of squirrel-cage induction generator and back-to-back PWM converter connected to the grid through the coupling inductances.

The voltage equations which describe the behavior of induction machine contain time-varying coefficients in real domain, due to the fact that some of the machine inductances are functions of the rotor displacement. A change of variables suggested by reference-frame theory is often used to reduce the complexity of these differential voltage equations [5]. It could be shown that in synchronously rotating reference frame a constant amplitude balanced 3-phase set of variables will appear as constants. This enables, among reduction of complexity of induction machine voltage equations and their analysis, also simplify in controlling the alternating systems because *ac* quantities became constants in steady-states. In system analysis it is also often convenient to express machine parameters and variables as per unit quantities. Base power and base voltage are

selected, and all parameters and variables are normalized using these base quantities. Modeling of induction machine was done in synchronously rotating reference frame (field oriented, also called  $dq$  reference frame) based on equations (2-5):

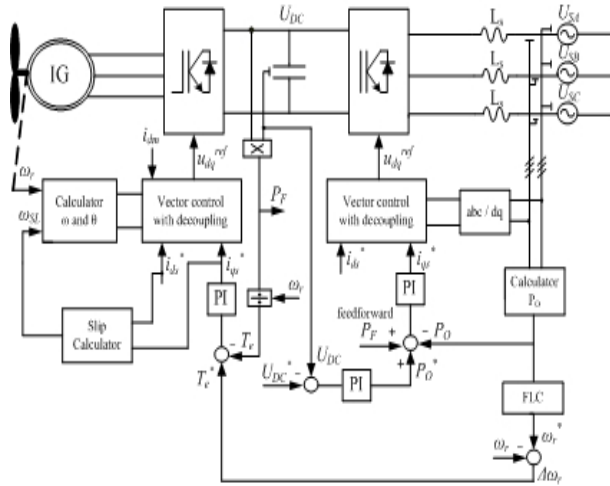


Figure 4

Power coefficient  $C_p(\lambda)$  related with tip-speed ratio  $\lambda$

$$\tau_{el} \cdot \frac{d\bar{i}}{dt} = \bar{u} - \bar{r} \cdot \bar{i} - \bar{Y}_1 \cdot \bar{\psi} \cdot \omega_e - \bar{Y}_2 \cdot \bar{\psi} \cdot \omega \quad (2)$$

$$\tau_{meh} \cdot \frac{d\omega}{dt} = m_c - m_m \quad (3)$$

$$m_c = x_m \cdot (i_{sq} \cdot i_{rd} - i_{sd} \cdot i_{rq}) \quad (4)$$

$$\bar{\psi} = \bar{x} \cdot \bar{i} \quad (5)$$

where are:

$$\bar{u}^T = [u_{sd} \quad u_{sq} \quad 0 \quad 0]$$

$$\bar{i}^T = [i_{sd} \quad i_{sq} \quad i_{rd} \quad i_{rq}]$$

$$\bar{\psi}^T = [\psi_{sd} \quad \psi_{sq} \quad \psi_{rd} \quad \psi_{rq}]$$

$$\bar{r} = [r_s, 0, 0, 0; \quad 0, r_s, 0, 0; \quad 0, 0, r_r, 0; \quad 0, 0, 0, r_r]$$

$$\bar{x} = [x_s, 0, x_m, 0; \quad 0, x_s, 0, x_m; \quad x_m, 0, x_r, 0; \quad 0, x_m, 0, x_r]$$

$$\bar{Y}_1 = [0, -1, 0, 0; 1, 0, 0, 0; 0, 0, 0, -1; 0, 0, 1, 0]$$

$$\bar{Y}_2 = [0, 0, 0, 0; 0, 0, 0, 0; 0, 0, 0, 1; 0, 0, -1, 0]$$

In the above equations the  $s$  subscript denotes variables and parameters associated with the stator circuits, and the  $r$  subscript denotes variables and parameters associated with the rotor circuits.  $d$  subscript denotes variables associated with vector component directed to  $d$ -axis of rotating reference frame, and  $q$  subscript denotes variables associated with vector component directed to  $q$ -axis of reference frame.  $u$  is the voltage vector,  $i$  is the current vector,  $\psi$  is the flux linkage vector,  $r$  is the machine resistances matrix,  $x$  is machine winding inductances matrix,  $x_m$  is the mutual inductance between stator and rotor windings i.e. magnetizing inductance,  $x_s$  and  $x_r$  among magnetizing inductance includes leakage inductances,  $\tau_{el}$  is electrical time constant of the machine ( $x_s/\omega_{base}$  or  $x_r/\omega_{base}$ ),  $\omega$  is the rotor speed,  $\omega_e$  is the angular speed of the rotating magnetic field,  $\tau_{meh}$  is mechanical time constant of the machine (together with the connected load, equals to  $J\omega_{base}/m_{base}$ , where  $J$  represents machine moment of inertia),  $m_c$  is the electromagnetic torque generated by the machine and  $m_m$  is the load torque. Based on the equations (2-5) model of the machine was made in MATLAB/Simulink, and it is shown in Fig. 5.

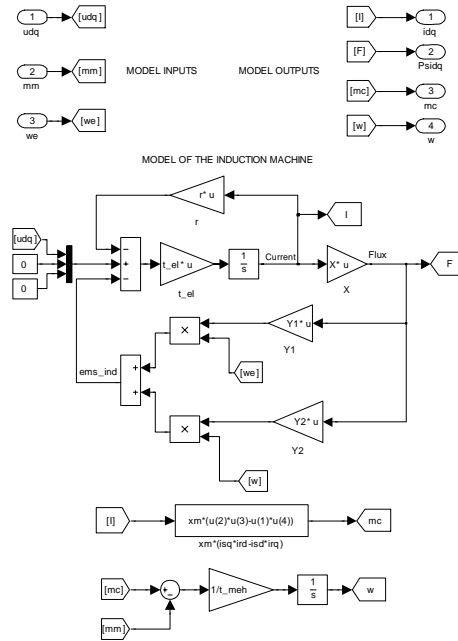


Figure 5

MATLAB/Simulink model of the induction machine

Back-to-back converter consists of two three-phase converters coupled through a common DC link. Generator side converter, i.e. rectifier, uses indirect field oriented or vector control in the inner current control loop. The aim of field-oriented control is to establish and maintain perpendicular relationship between the stator current space vector and usually rotor flux linkage vector. In this approach,  $d$ -axis of the rotating reference frame is aligned with the rotor flux vector,  $\psi_r$  ( $\psi_{rq}=0$ ). Under these conditions, the stator current component along  $q$ -axis,  $i_{sq}$ , defines machine electrical torque, whereas stator current component along  $d$ -axis,  $i_{sd}$ , defines machine flux linkage, similarly to a DC machine control. Field orientation can be achieved by on-line estimation of the rotor flux vector position based on next equations (6-9):

$$\theta_e = \int \omega_e \cdot dt \tag{6}$$

$$\omega_e = \omega + \omega_{slip} \tag{7}$$

$$\frac{\tau_{r\_el}}{r_r} \cdot \frac{d\psi_{rd}}{dt} + \psi_{rd} = x_m \cdot i_{sd} \tag{8}$$

$$\omega_{slip} = \frac{x_m}{\psi_{rd}} \cdot \frac{r_r}{x_r} \cdot i_{sq} \tag{9}$$

where are:

$\theta_e$  – electromagnetic field angular position,  $\omega_{slip}$  – slip angular frequency, and  $\tau_{r\_el}$  – electrical time constant of rotor windings ( $x_r/\omega_{base}$ ). By maintaining  $i_{sd}$  constant, the machine flux will be constant and  $i_{sq}$  will, in the case that Eq. (7) is fulfill, define motor torque which is expressed by equation (10):

$$m_c = \frac{3}{2} \cdot \frac{p}{2} \cdot \frac{x_m}{x_r} \cdot \psi_{rd} \cdot i_{sq} \tag{10}$$

where  $p$  represents number of poles of the machine. Blocks denoted in Fig. 4 as “slip calculator” and “calculator of  $\omega_e$  and  $\theta_e$ ” are implemented in MATLAB/Simulink based on Eqs. (6-9), and are shown in Fig. 6.

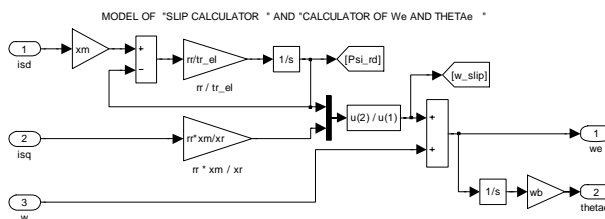


Figure 6  
MATLAB/Simulink model of the slip calculator

In general, output voltage of the voltage source converter,  $u_{abc}$ , can be expressed by defining a switching functions for each phase of the converter -  $S_{aN}$ ,  $S_{bN}$  and  $S_{cN}$ . Line-to-neutral output voltages of the converter then can be expressed as:

$$\begin{bmatrix} u_{aN} \\ u_{bN} \\ u_{cN} \end{bmatrix} = \begin{bmatrix} S_{aN} \\ S_{bN} \\ S_{cN} \end{bmatrix} \cdot u_{DC} \quad (11)$$

where  $u_{DC}$  represent *dc* voltage across dc-link capacitor *C*. Sequence of switching functions,  $S_{aN}$ ,  $S_{bN}$ , and  $S_{cN}$ , in order to achieve a 3-phase sinusoidal voltage waveforms without low-frequency harmonic content, is usually determined by space-vector pulse width modulation strategy (SVPWM). Advantage of SVPWM modulation strategy is that it is particularly designed to work with voltage commands expressed in terms of *dq* variables and it utilizes DC link voltage better compared to conventional sine PWM. Because this paper analyzes features of fuzzy logic speed controller of wind turbine machine, which is relative slow process, appearances on PWM level are neglected. Simply, average model of converter is used by defining the *d*- and *q*-axis modulation indexes (Eq. (12)):

$$d_d = \frac{u_d}{u_{dc}} \quad d_q = \frac{u_q}{u_{dc}} \quad (12)$$

Modulation indexes  $d_d$  and  $d_q$  represents average values of switching functions ( $S_{aN}$ ,  $S_{bN}$ , and  $S_{cN}$ ) over the PWM period, which are translated in *dq* domain. Voltage commands  $u_d$  and  $u_q$  are outputs of corresponding PI controllers (see Fig. (4)). In *dq* domain there is a coupling between the axes, i.e. in Eq. (2) term with  $i_q$  exists in equation for  $i_d$ , and reverse, term with  $i_d$  exists in equation for  $i_q$ . This circumstance complicates design of current controllers. By including feed-forward terms as part of the current controllers (axis decoupling), as it is shown in Fig. 7, controllers perceives machine electrical dynamic as a process that could be described by following first-order model:

$$G_i(s) = \frac{1/r_s}{1 + s \cdot (\tau_{s\_el}/r_s)} \quad (13)$$

Now, controller gains could be obtained easily, based on symetrical criterion as:

$$K_p = \frac{\sigma \cdot x_s}{\omega_{base} \cdot T_{sw}} \quad K_i = \frac{\sigma \cdot x_s}{2 \cdot \omega_{base} \cdot T_{sw}^2} \quad (14)$$

where are:

$\sigma$  – leakage constant ( $(1-x_s \cdot x_r/x_m^2)$ ), and  $T_{sw}$  – switching period (i.e. PWM period).



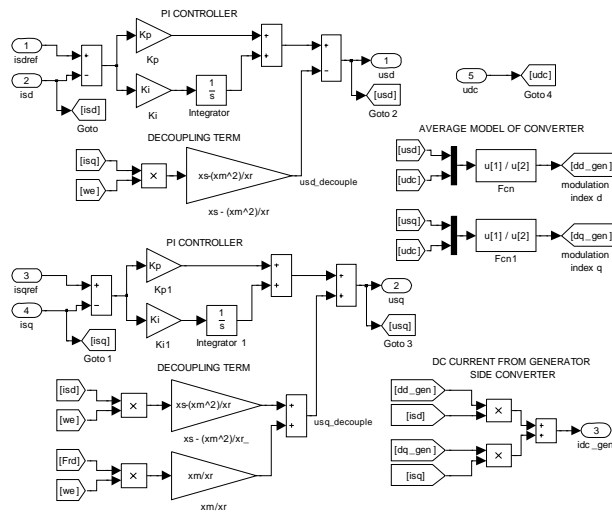


Figure 7

MATLAB/Simulink model of generator current controllers and generator side converter

Although changes of variables are used in the analysis of ac machines to eliminate time-varying inductances, changes of variables, i.e. reference-frame theory, are also employed in the analysis of constant-parameter power system and control system associated with them. So it is convenient to perform the grid side converter control design in synchronously rotating reference frame, where alternating variables become constants in the steady state.

In this approach, reference frame  $q$ -axis is aligned with the grid voltage vector,  $u_g$  ( $u_{gd}=0$ ). Grid voltage vector orientation could be achieved by directly measuring grid phase voltages, so this method is often called direct vector control. It could be shown that under this case, active power flow between grid side converter and the grid is determined with converter current in  $q$ -axis,  $i_{gq}$ , and reactive power flow is determined with converter current in  $d$ -axis,  $i_{gd}$ . It is obvious from Eqs. (15-16) providing that  $d$  voltage component is equal to zero.

$$p = u_{gd} \cdot i_{gd} + u_{gq} \cdot i_{gq} = u_{gq} \cdot i_{gq} \quad (15)$$

$$q = u_{gd} \cdot i_{gq} - u_{gq} \cdot i_{gd} = -u_{gq} \cdot i_{gd} \quad (16)$$

With the DC-link voltage maintained at fixed value, grid side converter controls active power flow so that all generated power is transferred to the grid. This is the reason why the DC voltage controller output is associated to the  $q$  current reference. In order to have an efficient DC-link voltage control, beside PI controller, it is needed to have feed forward signal of estimated output power in addition to the output of DC-link controller. In this way fluctuations of DC-link voltage are eliminated in transient periods. It could be noticed that increase of the

output power  $p_O$  ( $p_{grid}$ ) causes decrease of DC-link voltage  $u_{DC}$ , so the voltage loop error polarity has been inverted (see Fig. 4). DC-link voltage controller gives reference of the grid active power flow at his output. Grid active power is controlled with another PI controller which gives  $q$  current reference.  $d$ -current reference is set to zero, in order to have unity power factor. Decoupling is applied in both current control loops in order to have independent control of  $d$  and  $q$  current components. MATLAB/Simulink model of grid side converter, associated current controllers and power flow controllers are shown in Fig. 8.

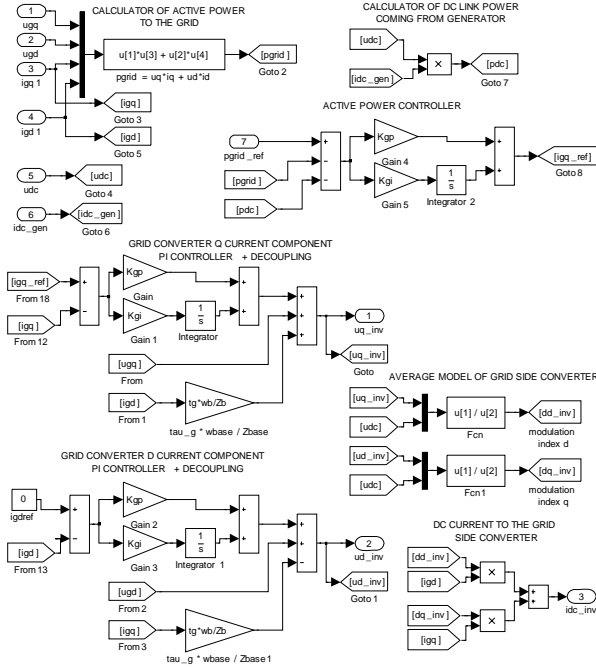


Figure 8

MATLAB/Simulink model of grid power and current controllers and grid side converter

Loop equation which describes grid side converter (connected to the grid) behavior in  $dq$  domain could be expressed as:

$$\tau_g \cdot \frac{d}{dt} \begin{bmatrix} i_{gd} \\ i_{gq} \end{bmatrix} = \begin{bmatrix} d_{gd} \\ d_{gq} \end{bmatrix} \cdot u_{DC} - \begin{bmatrix} 0 \\ u_{gq} \end{bmatrix} - r_g \cdot \begin{bmatrix} i_{gd} \\ i_{gq} \end{bmatrix} + \begin{bmatrix} 0 & \omega \\ -\omega & 0 \end{bmatrix} \cdot \begin{bmatrix} i_{gd} \\ i_{gq} \end{bmatrix} \quad (17)$$

where are:

$\tau_g$  – equivalent time constant of the grid ( $L_g/Z_{base}$ ),  $r_g$  – equivalent grid resistance ( $R_g/Z_{base}$ ),  $d_{gd}$  and  $d_{gq}$  – grid side converter modulation indexes, and  $\omega$  – grid frequency.

By applying decoupling of  $d$ - and  $q$ -axis, as noted in Fig. 8 and based on equation (17), grid side PI controller would perceive grid dynamic as a process that could be described by following first-order model:

$$G_{gi}(s) = \frac{1/r_g}{1 + s \cdot (\tau_g / r_g)} \quad (18)$$

Now, controller gains could be obtained easily, based on symmetrical criterion as:

$$K_{gp} = \frac{\tau_g}{2 \cdot T_{sw}} \quad K_{gi} = \frac{\tau_g}{4 \cdot T_{sw}^2} \quad (19)$$

The equation which describe voltage across DC-link capacitor  $C$  could be expressed by noticing that current through the capacitor is difference between dc current flowing from generator side converter,  $i_{dc\_gen}$ , and dc current flowing to the grid side converter,  $i_{dc\_inv}$ :

$$\tau_c \cdot \frac{du_{DC}}{dt} = i_{dc\_gen} - i_{dc\_inv} \quad (20)$$

where  $\tau_c$  represents equivalent time constant of DC-link ( $C \cdot Z_{base}$ ). dc currents of both converters could be calculated based on  $dq$  components of their phase currents and their  $dq$  modulation indexes (as denoted in Figs. 7 and 8):

$$i_{dc\_gen} = d_d \cdot i_{sd} + d_q \cdot i_{sq} \quad (21)$$

$$i_{dc\_inv} = d_{gd} \cdot i_{gd} + d_{gq} \cdot i_{gq} \quad (22)$$

Parameters gains for DC voltage controller are also set based on symmetrical criterion and they are calculated as:

$$K_{p\_dc} = \frac{\tau_c}{2 \cdot T_{dc}} \quad K_{i\_dc} = \frac{\tau_c}{4 \cdot T_{dc}^2} \quad (23)$$

where  $T_{dc}$  denotes DC voltage control loop period, and in this work it has been taken  $T_{dc} = 10 \cdot T_{sw}$ , because it is much slower process compared to the current control. Model of back-to-back converter DC link and DC voltage controller is shown in Fig. 9.

By appropriate connecting above described models, we have complete wind turbine model with reference generator speed as an input. Reference value of the generator speed would be set up by fuzzy logic speed controller with the aim to extract maximum power from available wind.

### 4 Fuzzy Logic Speed Controller

The optimum fuzzy logic control of an induction generator require controller which will track wind speed in order to achieve  $\lambda_{opt}$  and thus extract maximum power.

The product of torque and speed gives turbine power, and by assuming a steady-state lossless system it is equal to the grid power. The curves in Fig. 2 show the grid power  $p_o$  in dependence of generator speed  $\omega_r$  in terms of wind velocities  $v_w$ . What is the exact task of fuzzy controller it could be best seen from these set of power curves.

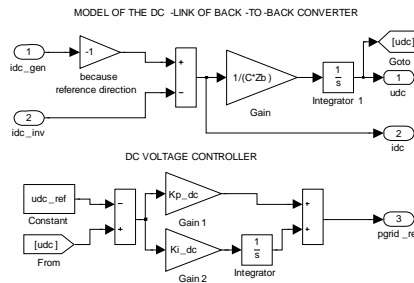


Figure 9  
MATLAB/Simulink model of the DC link and DC voltage controller

For a particular value of wind velocity, the function of the fuzzy controller FLC is to seek the generator speed in steps until the system settles down at the maximum output power operating point. For example, at a wind velocity of  $V_{w4}$ , the output power will be at point A if the generator speed is  $\omega_{r1}$ . The FLC will change the speed in steps until it reaches the speed  $\omega_{r2}$ , where the output power is maximized at point B. If the wind velocity increases to  $V_{w2}$ , the output power will jump to point C, and then FLC will bring the operating point to D by searching the generator speed to  $\omega_{r4}$ . The strategy for decrease of wind velocity is similar. If wind velocity decreases to  $V_{w3}$ , output power is altered and settled at operating point E. FLC will now decrease generator speed to the optimum value  $\omega_{r3}$  (point F) where output power is at maximum.

Therefore, the principle of the fuzzy controller is to increment or decrement the generator speed in accordance with the corresponding increment or decrement of the estimated output power  $p_o$ . If  $\Delta p_o$  is positive with the last positive  $\Delta \omega_r$ , the search is continued in the same direction. If, on the other hand, positive  $\Delta \omega_r$  causes negative change  $\Delta p_o$ , the direction of search is reversed. So, during these step changes of generator speed, controller observes changes in turbine output power and due to this it keeps searching generator speed for which this change of output power would be zero. That would be the maximum power delivery point. If  $\omega_{r1}$  is far from  $\omega_{r2}$ , controller could give greater value of generator speed

increments,  $\Delta\omega_r$ , for faster convergence to the maximum delivery point. Similar, if current generator speed is close to the  $\omega_{r2}$  controller must give smaller value of speed increments,  $\Delta\omega_r$ , to avoid oscillations and ensure stable system. Descriptive rules like this could be applied converting the system into the fuzzy system. Implemented control system is universal fuzzy control system, with block diagram shown in Fig. 10.

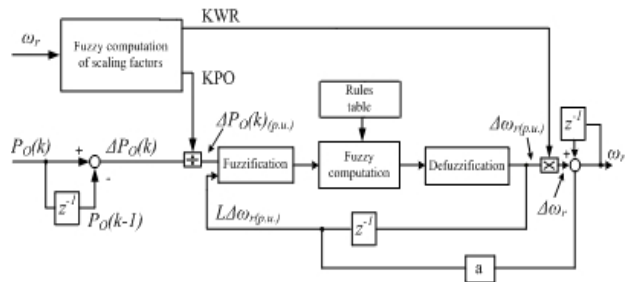


Figure 10

Block diagram of generator speed fuzzy controller

Actual values that indicates input variables, here change of output power,  $\Delta p_O$ , and last change of generator speed,  $L\Delta\omega_r$ , are initially converted into the correspondent fuzzy sets with human descriptive and intuitive values such are terms BIG, MEDIUM, SMALL, ZERO. This is done in the “fuzzification block”, where the variables  $\Delta p_O$  (variation of output power),  $\Delta\omega_r$  (variation of generator speed) and  $L\Delta\omega_r$  (last variation of generator speed) are described by membership functions given in Fig. 11. Afterwards, it is possible to apply descriptive rules of reasoning like “if the last change of output power  $\Delta p_O$  during maximum power searching was POSITIVE and BIG and the last change of desired generator speed  $L\Delta\omega_r$  was POSITIVE then keep tracking the maximum power in the same POSITIVE direction with BIG increment  $\Delta\omega_r$ ”. Rules like this are involved in block “rules table”, and they are given in Table 1. Finally, the fuzzy set of output reference change of generator speed  $\Delta\omega_r$  is back “defuzzified” to convert it to the actual value. That means the output values such are BIG, MEDIUM, SMALL are translated to numbers which indicates a measurable (but normalized) value of the generator speed. It could be also noticed the output of controller  $\Delta\omega_r$  is added by some amount of  $L\Delta\omega_r$  in order to avoid local minima in characteristics  $C_p(\lambda)$  due to the changes of wind speed. value. That means the output values such are BIG, MEDIUM, SMALL are translated to numbers which indicates a measurable (but normalized) value of the generator speed. It could be also noticed the output of controller  $\Delta\omega_r$  is added by some amount of  $L\Delta\omega_r$  in order to avoid local minima in characteristics  $C_p(\lambda)$  due to the changes of wind speed.

The controller operates on a per-unit basis so that the response is insensitive to system variables and the algorithm is universal to any system. Membership functions of FLC controller are implemented by using MATLAB/Simulink fuzzy

control toolbox. In Fig. 12 realized model of fuzzy logic controller is shown. Heart of the controller is block of fuzzy logic controller from MATLAB/Simulink fuzzy control toolbox. With this powerful tool it is possible to define your fuzzy controller in relatively easy way using graphical interface and intuitive dialogs, which is obvious from Figs. 13 and 14.

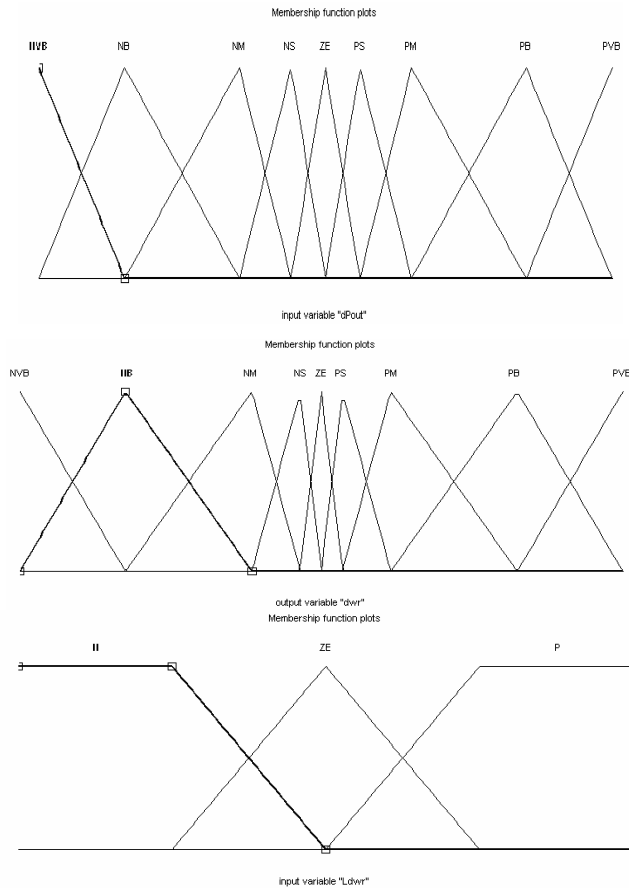


Figure 11

Membership functions for fuzzy controller ( $\Delta P_o$ ,  $\Delta \omega_r$ , and  $L\Delta \omega_r$ , respectively)

In Fig. 10 could be noted scaling factors  $KPO$  and  $KWR$ . The scale factors  $KPO$  and  $KWR$  are functions of the generator speed, so that control becomes somehow insensitive to speed variation. The scale factors are generated by fuzzy computation realized in *Matlab/Simulink* as shown in Fig. 15. Their values are generated partly empirically, and partly taking into account dependence of wind turbine power related to wind speed in terms of different generator speed.

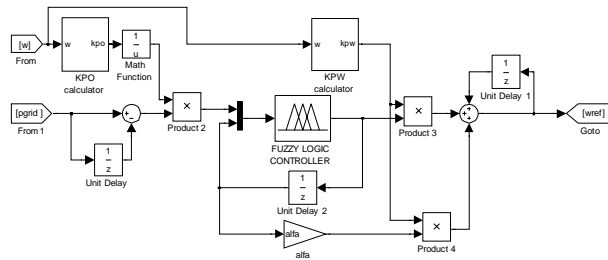


Figure 12  
MATLAB/Simulink model of fuzzy logic controller

Table 1  
Rules table for the fuzzy controller

$\Delta\omega_r$ / $\Delta P_o$	<i>P</i>	<i>ZE</i>	<i>N</i>
<i>PVB</i>	<i>PVB</i>	<i>PVB</i>	<i>NVB</i>
<i>PBIG</i>	<i>PBIG</i>	<i>PVB</i>	<i>NBIG</i>
<i>PMED</i>	<i>PMED</i>	<i>PBIG</i>	<i>NMED</i>
<i>PSMA</i>	<i>PSMA</i>	<i>PMED</i>	<i>NSMA</i>
<i>ZE</i>	<i>ZE</i>	<i>ZE</i>	<i>ZE</i>
<i>NSMA</i>	<i>NSMA</i>	<i>NMED</i>	<i>PSMA</i>
<i>NMED</i>	<i>NMED</i>	<i>NBIG</i>	<i>PMED</i>
<i>NBIG</i>	<i>NBIG</i>	<i>NVB</i>	<i>PBIG</i>
<i>NVB</i>	<i>NVB</i>	<i>NVB</i>	<i>PVB</i>

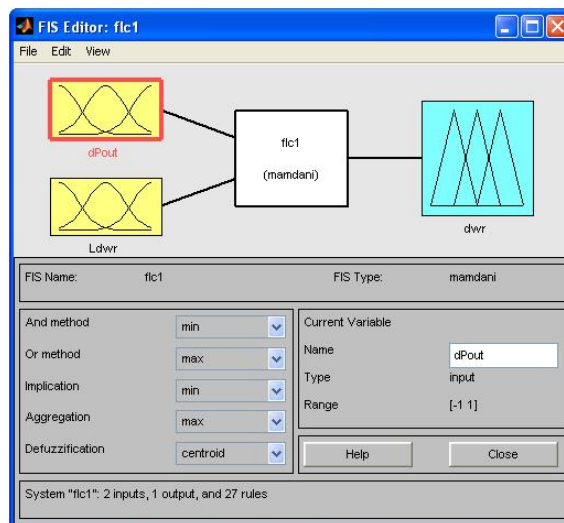


Figure 13  
MATLAB graphical editor for defining of fuzzy logic controller

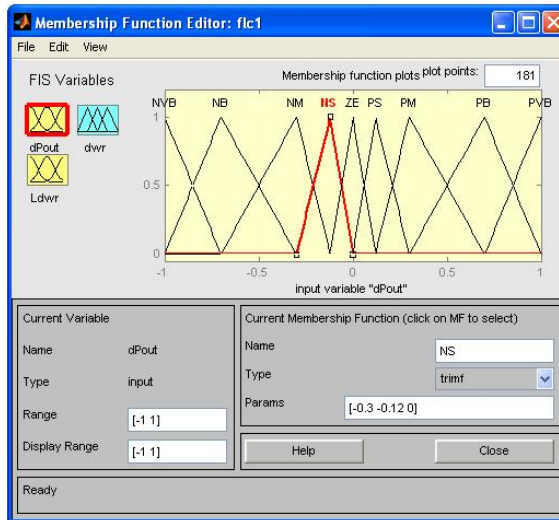
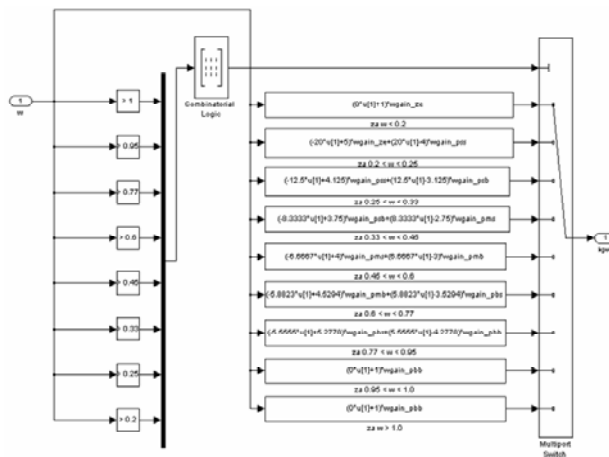


Figure 14

MATLAB graphical editor for defining membership functions of fuzzy logic controller

From previously explanations, the advantages of fuzzy control are obvious. It provides adaptive step size in the search that leads to fast convergence, and controller can accept inaccurate and noisy signals. The FLC operation does not need any wind velocity information, and its search is insensitive to system parameter variation which is helpful in installation of different scale wind turbines.





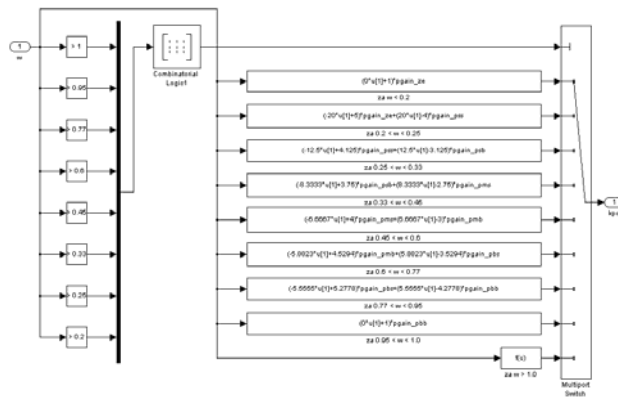


Figure 15

Implementation of membership functions for computation of scaling factors  $KWR$  and  $KPO$

## 5 Simulation Results

In order to verify control principle given in this paper, detailed model of the system in MATLAB/Simulink has been developed. The system data are shown in Table 2. Simulation results shown in Figs. 16 and 17 illustrate performance of wind turbine with fuzzy controller which tracks the maximum power delivery operating point. They are given for the case of wind velocity decrease from nominal to 80% of nominal value. It could be noticed that before disturbance ( $t < 5$  s) all variables are settled at nominal values. After wind velocities decrease power fed to the grid gradually decrease to value around 50% of nominal, which is expected because turbine power follows the cube law. Reference value of  $q$  current component  $i_{sq}$  also drops, and thus the value of electromagnetic torque.  $d$  current component  $i_{sd}$  remain the same, so the magnetic flux is unchanged. DC-link voltage is maintained constant which means that all generated power is transferred to the grid. Generator rotational speed is changing consistent with changes of wind velocity. Speed response is without overshoot and abrupt transients, as a consequence of fuzzy controller usage.

In order to verify that maximum power is extracted from the available wind, power coefficient  $C_p(\lambda)$  has to be observed. In Fig. 17,  $C_p(\lambda)$  is shown during the change of wind velocity.

It could be noticed that during the change of wind velocity, power coefficient  $C_p(\lambda)$  differs from optimum value. Deviation is relatively small, but after the transient period which lasts around 10 s, it settles at the optimum value.

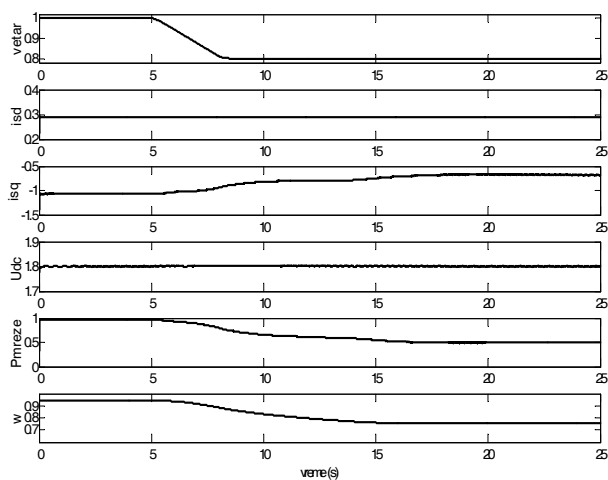


Figure 16

Simulation results. From up to down: wind velocity  $V_w$ ,  $d$  grid current component  $i_{sd}$ ,  $q$  grid current component  $i_{sq}$ , DC link voltage  $U_{DC}$ , grid power  $P_O$ , and generator speed  $\omega_r$

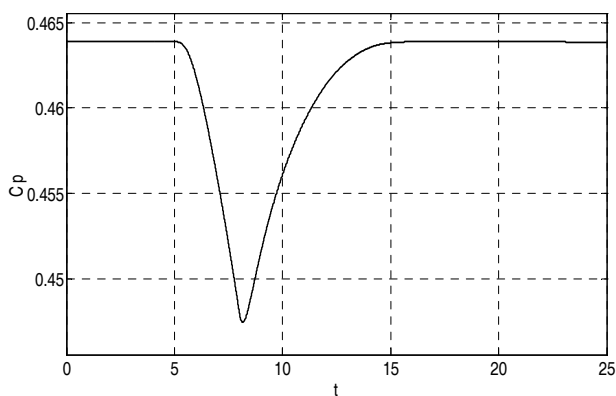


Figure 17

Power coefficient  $C_p(\lambda)$  during simulation

Table 2

The system parameters used in simulation

Stator resistance, $r_S$	7,7m (p.u.)
Rotor resistance, $r_R$	9,0m (p.u.)
Stator reactance, $x_S$	3,56 (p.u.)
Rotor reactance, $x_R$	3,53 (p.u.)
Magnetization reactance, $x_M$	3,47 (p.u.)
Leakage coefficient, $\sigma$	41m (p.u.)
Based angular speed, $\omega_B$	$100\pi$ rad/s

Grid resistance, $r_{GRID}$	6,4m (p.u.)
Grid reactance, $x_{GRID}$	40m (p.u.)
Fuzzy controller sampling per., $T_{flc}$	0,014 s
Capacitance of DC-link, $C$	1000 $\mu$ F
Based impedance, $Z_B$	16 $\Omega$
Turbine power coefficient, $C_{pMAX}$	0,4639

## Conclusion

In this paper optimum fuzzy control of wind turbine in order to extract maximum power is described and verified through the simulation. The main goal of implemented fuzzy controller is to continuously adapt the rotational speed of the generator to the wind speed in a way that the turbine operates at its optimum level of aerodynamic efficiency. The advantages of using fuzzy controller are universal control algorithm, fast response, and parameter insensitivity. Implemented system has satisfactory dynamic and static performances.

## References

- [1] Simoes, M. G., Bose, B. K., Spiegel, R. J., Fuzzy Logic-based Intelligent Control of a Variable Speed Cage Machine Wind Generation System, *IEEE Transactions on Power Electronics*, Vol. 12, pp. 87-95, Jan. 1997
- [2] Simoes, M. G., Bose, B. K., Spiegel, R. J., Design and Performance Evaluation of a Fuzzy Logic-based Variable Speed Wind Generation System, *IEEE Transactions on Industry Applications*, Vol. 33, pp. 956-965, July/August. 1997
- [3] E. Adžić, Z. Ivanović, M. Adžić, V. Katić, „Optimum Fuzzy Control of Induction Generator in Wind Turbine Application“, *6<sup>th</sup> International Symposium on Intelligent Systems and Informatics - SISY 2008*, Subotica, Serbia, Sept. 2008
- [4] Z. Ivanović, M. Vekić S. Grabić, V. Katić, “Control of Multilevel Converter Driving Variable Speed Wind Turbine in Case of Grid Disturbances”, *12<sup>th</sup> Inter. Power Electr. and Motion Control Conf. - EPE-PEMC 2006*, Portoroz, Slovenia, Aug. 2006
- [5] M. Vekić, Z. Ivanović, S. Grabić, V. Katić: “Control of Variable Speed Wind Turbine Under Grid Disturbances”, *13<sup>th</sup> International Symposium on Power Electronics – Ee 2005*, Novi Sad (S&M), Nov. 2005, Paper No. T7-1.1, ISBN 868521155-7, CD-ROM
- [6] Krause, P. C., Wasynczuk, O., Sudhoff S. D., *Modern Analysis of Electric Machinery and Drive Systems*, John Wiley and Sons, New York, 2002
- [7] Bose, B. K., *Modern Power Electronics and AC Drives*, Prentice Hall, New York, 2001